Louisiana State University
LSU Digital Commons

Faculty Publications | Department of Physics & Astronomy

11-1-2016

One-pot melamine derived nitrogen doped magnetic carbon nanoadsorbents with enhanced chromium removal

Yonghai Cao
The University of Tennessee, Knoxville

Jiangnan Huang
The University of Tennessee, Knoxville

Yuhang Li
South China University of Technology

Song Qiu
Shandong University

Jiurong Liu
Shandong University

See next page for additional authors

Follow this and additional works at: https://digitalcommons.lsu.edu/physics_astronomy_pubs

Recommended Citation

Cao, Y., Huang, J., Li, Y., Qiu, S., Liu, J., Khasanov, A., Khan, M., Young, D., Peng, F., Cao, D., Peng, X., Hong, K., & Guo, Z. (2016). One-pot melamine derived nitrogen doped magnetic carbon nanoadsorbents with enhanced chromium removal. *Carbon, 109*, 640-649. https://doi.org/10.1016/j.carbon.2016.08.035

This Article is brought to you for free and open access by the Department of Physics & Astronomy at LSU Digital Commons. It has been accepted for inclusion in Faculty Publications by an authorized administrator of LSU Digital Commons. For more information, please contact ir@lsu.edu.

Authors

Yonghai Cao, Jiangnan Huang, Yuhang Li, Song Qiu, Jiurong Liu, Airat Khasanov, Mojammel A. Khan, David P. Young, Feng Peng, Dapeng Cao, Xiangfang Peng, Kunlun Hong, and Zhanhu Guo

This article is available at LSU Digital Commons: https://digitalcommons.lsu.edu/physics_astronomy_pubs/5827

One-Pot Melamine Derived Nitrogen Doped Magnetic Carbon Nanoadsorbents with Enhanced Chromium Removal

Yonghai Cao,[1,2] Jiangnan Huang,[1,2] Yuhang Li,[3] Song Qiu,[4] Jiurong Liu,[4] Airat Khasanov,[5] Mojammel A Khan,[6] David P. Young,[6] Feng Peng,[3] Dapeng Cao,[7] Xiangfang Peng,[2] Kunlun Hong[8] and Zhanhu Guo[1*]

[1] Integrated Composites Laboratory (ICL), Department of Chemical and Biomolecular Engineering, University of Tennessee, Knoxville, TN 37996, USA

[2] Laboratory of Polymer Processing Engineering of Ministry of Education, South China University of Technology, Guangzhou, Guangdong 510640, P.R. China

[3] School of Chemistry and Chemical Engineering, South China University of Technology, Guangzhou, Guangdong, 510640, P.R. China

[4] School of Materials Science and Engineering, Shandong University, Jinan, Shandong, 250061, P.R. China

[5] University of North Carolina at Asheville, Asheville, NC 28804, USA

[6] Department of Physics and Astronomy, Louisiana State University, Baton Rouge, LA 70803, USA

[7] Division of Molecular and Materials Simulation Key Lab for Nanomaterials, Beijing University of Chemical Technology, Beijing, 100029, P.R. China

[8] Center for Nanophase Materials Sciences, Oak Ridge National Laboratory, Oak Ridge, TN 37831, USA

*Corresponding authors: Email: zguo10@utk.edu; Tel: +1 (865) 974-2933 (Zhanhu Guo)

© 2016. This manuscript version is made available under the Elsevier user license
http://www.elsevier.com/open-access/userlicense/1.0/

Abstract: Novel nitrogen doped magnetic carbons (NMC), in-situ synthesized through facile pyrolysis-carbonization processes using $Fe(NO_3)_3$ and melamine as precursors, were demonstrated as excellent nanoadsorbents to remove Cr(VI) effectively. The achieved removal capacity in both neutral and acidic solution was 29.4 and 2001.4 mg g^{-1} respectively, much higher than the reported adsorbents so far. The unprecedented high adsorption performance can be attributed to the incorporation of the nitrogen dopant, which increased the negative charge density on the surface of adsorbent and thereby enhanced the interaction betweent the adsorbents and Cr(VI) ions. The density functional theory (DFT) calculation demonstrated that the nitrogen dopants can decrease the adsorption energy between the Cr(VI) ions and NMC (-3.456 kJ mol^{-1}), lower than the undoped sample (-3.344 kJ mol^{-1}), which boosted the adsorption behavior. Chemical rather than physical adsorption was followed for these magnetic nanoadsorbents as revealed from the pseudo-second-order kinetic study. Furthermore, the NMC showed high stability with recycling tests for the Cr(VI) removal.

1. Introduction

Environmental pollution has become an urgent issue for our society caused by the rapid industrialization [1]. Heavy metal ion Cr(VI) is a typical contaminant for its wide industrial applications. Herein, it is crucial to remove Cr(VI) ions from the waste water due to its high toxicity and mobility [2]. Adsorption was considered as a conventional and effective process because of its simple operation without producing by-products, thus avoiding secondary pollution [3, 4]. Among the reported adsorbents, such as biosorbents, clay minerals, metal phosphates, zeolites, activated carbon, and magnetic carbons [5-12]. Magnetic carbons become popular due to their highly porous structure with easily-controlled chemical properties and magnetization for easy separation [4, 10, 11, 13-15]. For example, Lv and coworkers reported a maximum Cr(VI) removal capacity (q_{max}) of 101.0 mg g^{-1} (pH is 3) for the nano zero-valence iron (ZVI) assembled on magnetic Fe_3O_4/graphene nanocomposites, due to strong adsorption capability of broad graphene sheet/Fe_3O_4 surfaces and the redox reaction between ZVI and Cr(VI) ions [16]. However, this removal efficiency is still not enough for the heavy metal uptake.

The doping of carbon materials with heteroatoms such as nitrogen and sulfur et al. has attracted considerable attention in the environment remediation [17-21]. Heteroatom dopants can endow adsorbents unique electronic features and rich function groups on the surface, thus change the adsorption efficiency for removing heavy metal ions. Recently, the usage of nitrogen doped carbons as adsorbents in the Cr(VI) removal received increasing attentions, since the nitrogen atom has higher electronegativity than carbon atom, thus increasing the negative charge density and the amount of higher basicity functionalities on the surface of adsorbent, facilitating the adsorption ability of metal ions [18, 20, 22-24]. For example, Shin and his co-workers reported [19] that the nitrogen doped carbon composites with iron nanoparticles prepared by using pyrrole and ferric chloride as precursors demonstrated great

active sites for the Cr(VI) adsorption. The adsorption onto nitrogen doped magnetic carbon composites occurred through a chemical process involving valence forces. The Cr(III) adsorption capacity of nitrogen doped magnetic carbons was 10 folds higher than that of active carbons [19]. Although great efforts have been made for the nitrogen doped adsorbent to enhance Cr(VI) removal, two essential problems still remain in the nitrogen doped adsorbents for Cr(VI) removal: firstly, detailed evidence to confirm the influence of nitrogen dopant on the Cr(VI) removal efficiency is not reported; secondly, how the N dopants changing the efficiency of Cr(VI) removal by modulating the electronic structure of the adsorbent surface is far from understood.

In this work, nitrogen doped magnetic carbons (NMC) with controlled nitrogen doping levels were synthesized through a facile one-step thermal pyrolysis method using melamine as both carbon and nitrogen sources. The influences of Cr (VI) concentration, adsorbents loading, adsorption time, pH and the adsorption kinetics were investigated in details. The Cr(VI) removal performances were studied based on the physical and chemical properties of nanoadsorbents. The relationship between nitrogen doping and Cr(VI) removal was established. Both kinetics and isothermal analysis were used to disclose the Cr(VI) removal mechanisms. Theoretical simulation by using density functional theory (DFT) based on the interaction between Cr(VI) and adsorbent was conducted to understand the enhancement of nitrogen dopant for the Cr(VI) removal.

2. Experimental

2.1 *Materials*

Potassium dichromate (99%, $K_2Cr_2O_7$), 1,5-diphenylcarbazide (97%, DPC) and denatured ethanol (92.2%) were purchased from Alfa Aesar Company. $Fe(NO_3)_3 \cdot 9H_2O$ (99%), sodium hydroxide (NaOH, 99.1%), sulfuric acid (H_2SO_4, 95%), phosphoric acid (H_3PO_4, 85%),

melamine (99%) and glucose (99%) were obtained from Fisher Scientific. All the chemicals were used as received without any further purification.

2.2 *Synthesis of nitrogen doped magnetic carbon nanoadsorbents*

The nitrogen doped magnetic carbon nanoadsorbents were synthesized as follows. Typically, 6 g $Fe(NO_3)_3 \cdot 9H_2O$ and 3 g melamine were added into denatured alcohol solvent and then treated under ultrasonication for 2 h to be intensively mixed. After that, the mixture was dried at 110 ^oC overnight. The obtained solid sample was then carbonized at 800 ^oC for 2 h under N_2 atmosphere. To control the nitrogen doping levels, glucose was added into mixture to adjust the melamine concentration at 0, 33, 50, 66 and 100 wt%, which was noted as the NMC-0, NMC-33, NMC-50, NMC-66 and NMC-100, respectively, in the following.

2.3 *Characterizations*

Transmission electron microscope (TEM) images were obtained with a FEI Tecnai G2 12 microscope operated at 100 kV. The samplse were prepared by ultrasonically suspending in acetone and depositing several drop of the suspension onto a grid. Scanning electron microscope (SEM) images were obtained with a FEI Quanta 600F electron microscope. X-ray diffraction (XRD) patterns were obtained from a Bruker D8 ADVANCE diffractometer equipped with a rotating anode using Cu Kα radiation (40KV, 40mA). X-ray photoelectron spectroscopy (XPS) were performed in a Kratos Axis ultra (DLD) spectrometer equipped with an Al Kα X-ray source in ultrahigh vacuum (UHV) ($<10^{-10}$ Torr). Brunauer-Emmett-Teller (BET) specific surface areas were measured by N_2 adsorption at liquid N_2 temperature in an ASAP 2010 analyzer. The magnetic property measurements were conducted in a 2 T physical property measurement system (PPMS) by Quantum Design at room temperature. The thermogravimetric analysis (TGA) was carried out on a NETZSCH TGASTA 409 PC analyzer.

2.4 *The Cr(VI) removal performance of NMCs*

Typically, the selected nanoadsorbents were added into the Cr(VI) solution and treated under ultrasonication for certain time at room temperature. The Cr(VI) removal efficiency based on the effects of different Cr(VI) concentration (from 1.0 to 150 mg L^{-1}), nanoadsorbents loading (from 0.5 to 5 g L^{-1}), treatment time (from 2.5 to 10 min) and pH value (from 1.0 to 11, measured by a pH meter, Vernier Lab Quest with pH-BTA sensor) were studied in details.

2.5 *Computational Simulations*

The adsorption properties were investigated by spin-polarized density functional theory (DFT) calculations with DMol3 package. Exchange-correlation functions were described by GGA/PBE. The electronic basis set was double numerical plus polarization (DNP) set, which was equal to 6-31G** in Gaussian [25]. The "DFT semi-core pseudopots (DSPPs)" method was adopted as the core treatment. The orbital cutoff with 5.0 Å was set for all atoms. To avoid the shortage of handling weak interactions by DFT, the long range dispersion was corrected by the Grimme scheme. The conductor-like screening model (COSMO) with the permittivity of 78.54 (water) was considered to mimic structures encased by the aqueous layer [26]. It is essential to extract a simplified model as the initial structure in DFT calculations. The primitive hexagonal graphene cell was extended to a (4×4×1) supercell with the optimized parameters of 9.84 Å × 9.84 Å × 25 Å, where the extension along c axis represented the elimination of interactions between adjacent layers. The k-point was set to 8×8×1 after convergence tests. We assumed that Cr(VI) existed as a form of CrO_4^{2-} cluster with two negative charges. The adsorption energy (E_{ads}) was calculated as the formula below:

$$Eads=E(X\cdots CrO_4^{2-})- E(X)- E (CrO_4^{2-})$$

where, $E(X\cdots CrO_4^{2-})$ is the energy of the steady adsorption state on different adsorbents; E(X) is the energy of the isolated adsorbent; $E(CrO_4^{2-})$ is the energy of the isolated adsorbate CrO_4^{2-} cluster.

3. Results and discussion

3.1 *Physical/chemical properties of nitrogen doped magnetic carbons.*

Figures 1a-e display the typical SEM images of magnetic carbons in all the samples prepared at 800 ^{o}C in N_2 atmosphere. Large amount of mesoporous carbon are observed and some nanospheres are interconnected but with non-uniform distribution. Figures 1f-j show the TEM images of the NMCs, further revealing the interconnected nanospheres and the core-shell structure in all the samples. The undoped magnetic carbons (NMC-0) displayed relatively uniform particle of ~80 nm (Figure 1f). However, non-uniform larger core-shell particles from 50~160 nm were observed after the addition of melamine (Figure 1g to j), which can be attributed to the aggregation of Fe particles during the pyrolysis and carbonization of melamine. The carbon coating for the NMC-0 was about 3-5 nm, which was also observed in the Fe_3O_4 nanocrystals synthesized by the hydrothermal method with glucose as carbon source [27]. For the NMCs, the bouffant structure of carbon layer was observed and attributed to the nitrogen doping. Nitrogen doped carbon nanotubes (NCNTs) with typical bamboo structure in the NMC-100 was also observed (Figure 1k) arising from the high mobility of melamine during the synthesis of NMCs [28, 29]. The XRD patterns show four kinds of iron state existing in all the samples (Figure 2). The abundance of ZVI nanoparticles was observed, demonstrating that the Fe_3O_4 or Fe_2O_3 were partially reduced by the glucose or melamine during the calcination process [4], which was also observed in the Mössbauer spectra (Figure S1). The intensity ratio of Fe_3O_4 to ZVI on any NMC was higher than that of the NMC-0, indicating that Fe^{3+} can be more favorably transformed to the ZVI with the addition of melamine as the precursor.

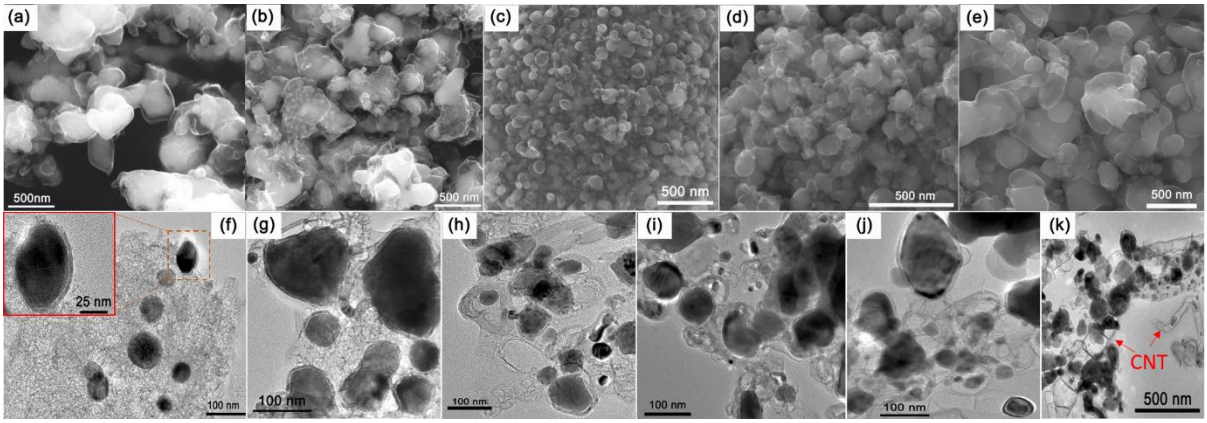

Figure 1. The SEM (a-e) and TEM (f-k) images of magnetic adsorbents: (a and f) for NMC-0; (b and g) for NMC-33; (c and h) for NMC-50; (d and i) for NMC-66; (e, j and k) for NMC-100.

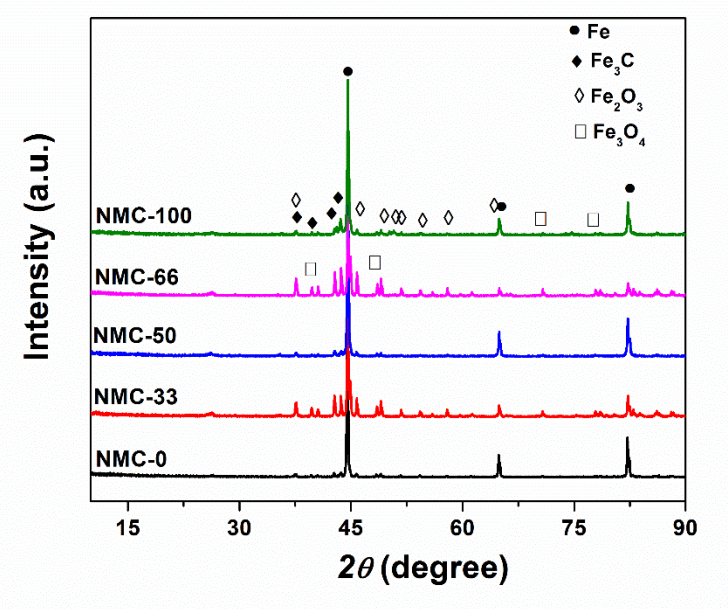

Figure 2. XRD patterns of magnetic adsorbents used in this study.

The nitrogen contents of the doped magnetic carbons were measured by XPS. As shown in Figures S2 and 3, the nitrogen atoms were successfully incorporated in the carbon skeleton. The contents of elements are summarized in Table S1, while Table 1 provides the detailed information about the N functionalities obtained from the deconvoluted N_{1s} XPS spectra. With increasing the melamine loading, the N/(N+C) atomic ratio increased from 0 to 4.9 %. Five nitrogen components were obtained from the spectra, representing pyridinic N, pyrrolic N,

quaternary N, Noxides and chemisorbed N, respectively [30-34]. The major functionalities of NMCs were pyridinic, pyrrolic and quaternary nitrogens. The pyrrolic nitrogen dramatically increased from 0 to 59.7 % with the addition of 33 wt% melamine, much higher than pyridinic and quaternary N. When the addition of melamine reached equal to or over 50 wt%, the percentages of pyridinic and quaternary nitrogens increased while pyrrolic nitrogen displayed a slight decrease, demonstrating that the higher melamine loading efficiently led to higher amount of pyridinic and quaternary N.

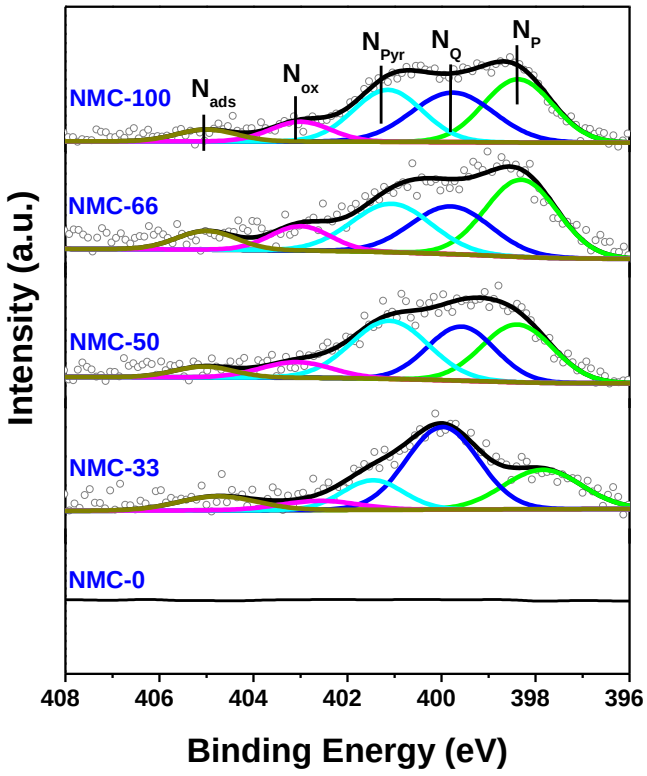

Figure 3. N_{1s} XPS spectra of the magnetic adsorbents used in this work.

Table 1 Quantitative XPS analysis of the NMCs. N_P: pyridinic N, N_{Pyr}: pyrrolic N, N_Q: quaternary N, N_{OX}: Noxides, N_{ads}:chemisorbed N.

Adsorbents	N/(N+C)(%)	N_P(%) 398 eV	N_{Pyr}(%) 400 eV	N_Q(%) 401.5 eV	Nox(%) 403 eV	N_{ads} (%) 405 eV
NMC-0	0	0	0	0	0	0

NMC-33	2.1	17.4	59.7	12.1	4.8	6
NMC-50	3.0	37.7	24.4	31.3	3.4	3.2
NMC-66	4.2	34.4	21.2	31.9	6.2	6.3
NMC-100	4.9	39.8	24.2	27.8	4.7	3.6

Figure 4 shows the Raman spectra of NMCs. According to previous work, the introduction of N heteroatoms can dramatically change the height and width of D band, due to the increasing disorder degree of graphene layers with N doping [34]. Apparently broadened G and D bands of these nitrogen doped magnetic carbons can be attributed to the enhanced vibrations from I (1166 cm^{-1}) bands and D' (1600 cm^{-1}) and D'' (1490 cm^{-1}) [35]. 5 peaks, i.e. G (1560 cm^{-1}), D (1320 cm^{-1}), D' (1600 cm^{-1}), D'' (1490 cm^{-1}) and I (1166 cm^{-1}) bands, were fitted in the nitrogen doped magnetic carbons. The intensity ratio based on D to G band (I_D/I_G) was used to evaluate the defective degree of NMCs. The NMC-0 displayed low defects degree (0.12) with narrow peak. The I_D/I_G of NMC-0 is 0.12, demonstrating that this sample has highly graphitized surface [27]. For the nitrogen doped samples, the I_D/I_G ratio gradually decreased from 2.44 to 1.25 with increasing the nitrogen content from 2.1% to 4.9%, totally different from the observation on the NCNT synthesized in the Ar atmosphere [34]. It may be attributed to the decomposition of melamine with the resultant formation of NH_3, which can be further decomposed into H_2, facilitating the removal of amorphous carbons deposited on the surface of carbons [34, 36].

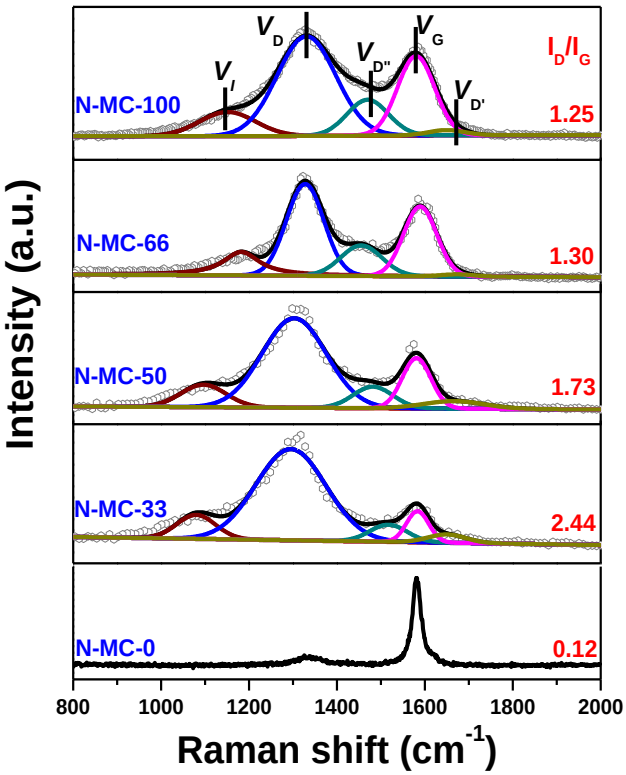

Figure 4. Raman spectra of magnetic adsorbents used in this work.

3.2 *Cr(VI) removal performance*

The specific surface area and Cr(VI) removal performance of different adsorbents are summarized in Table 2. The addition of undoped samples (MC) displayed reletively lower efficiency in the Cr(VI) removal, 30.7% removal percentage with the Cr(VI) initial concentration at 20 mg L^{-1}. After nitrogen doped (with 4.9% N content, see Figure 2 and Table 1), the Cr(VI) removal was greatly boosted to 100% removal percentage after 10 min ultrasonic treatment, corresponding to a mass removal rate of 3.2 mg g^{-1} min^{-1}, which was about 3 times higher than the undoped one. In this study, the mass and surface areas removal rate were directly defined by $\Delta C/(\Delta t \cdot m)$ or $\Delta C/(\Delta t \cdot S)$, not the Pseudo-second-order model or other models [11, 14]. Because these models are srongly depended on initial concentration of metal ions [37-39], which is not comparable for the adsorbents under different treatment systems. This removal capacity of NMC was comparable to the state-of-the-art magnetic adsorbent

reported before, such as magnetic carbon (0.008 mg g^{-1} min^{-1}) and reported N doped porous carbons (Fe and Ni based, 0.063 and 0.004 mg g^{-1} min^{-1}, respectively) [4, 18, 20]. There were two possible reasons. The first one is due to the abundent iron particles on the adsorbent surface, Figures 2 and S4. The existing iron particles on the surface played a significant role in the redox reaction with Cr(VI) ions [4, 11]. The second reason was due to the NCNTs enclosed with iron oxide synthesized (Figure 1k). The NCNTs could increase the surface areas, and thus created more active sites to adsorb Cr(VI) ions by the NMC. It may be argued that the iron nanoparticles on the surface may be play the signicifant role for the Cr(VI) removal in the neutral sulotion. Therefore, the NMC adsorbent was washed by concentrated HCl sulotion for 4 h. Around 82.5% removal percentage was obtained, indicating that the iron nanoparticles were not the dominat factor for the Cr(VI) remvoal in the neutral sulotion.

Table 2 The performance comparison of NMCs in the Cr(VI) removal.[a]

Entry	Adsorbents	S_{BET} [b] (m^2 g^{-1})	X[c](%)	r_g [d] (mg g^{-1} min^{-1})	r_s[e] (mg m^{-2} min^{-1})
1	MC[f]	21.7	30.7	0.980	0.041
2	NMC[g]	56.2	100	3.200	0.057
3	NMC-w[h]	–	82.5	–	–
4	Magnetic Carbons (Cellulose)[i]	111.4	100	0.008	7.000×10^{-4}
5	N-doped porous carbon (Fe)[j]	1136.0	92	0.063	5.586×10^{-5}
6	N-doped porous carbon (Ni)[k]	2148.4	100	0.004	1.862×10^{-6}

[a] Condition: [Cr (VI)] = 20 mg L^{-1}, pH = 7.0, adsorbent dosage: 50.0 mg, volume: 20 mL, treatment time: 10 min; [b] BET specific surface area, pore size and other dates can be obtained from Figure S3 and Table S2; [c] X: removal percentages; [d] Removal rate of Cr(VI) per gram of adsorbent based on the treatment of 2.5 min. [e] Removal rate of Cr(VI) per m^2 of catalyst surface based on the treatment of 2.5 min; [f] MC is represented as NMC-0; [g] NMC is represented as NMC-100; [h] NMC was washed by concentration HCl for 4 h; [i] Condition: [Cr (VI)] = 4 mg L^{-1}, pH = 7.0, adsorbent dosage: 50.0 mg, volume: 20 mL, treatment time: 10 min (ref. [4]); [j] Condition: [Cr (VI)] = 31.73 mg L^{-1}, pH = 3, adsorbent dosage: 2 g L^{-1}, treatment time: 10 min (ref. [18]); [k] Condition: [Cr (VI)] = 6 mg L^{-1}, pH = 2.5, adsorbent dosage: 0.05 g L^{-1}, treatment time: 30 min (ref. [20]).

Based on the aforementioned discussion, NMC is superior for the Cr(VI) removal. Herein, the NMC was used as the adsorbent to investigate the effect of initial Cr(VI) concentration, adsorbent dose, treat time and pH on the Cr(VI) removal efficiency. Figure 5a shows the Cr(VI) removal performance with different Cr(VI) concentrations by NMC in the neutral solution. Up to 20 mg L^{-1}, Cr(VI) could be completely removed by 2.5 g L^{-1} NMC in 10 min. This high Cr(VI) removal rate can be attributed to the abundant active sites on the NMC surface. The removal activity decreased with further increasing the Cr(VI) concentration from 40 mg L^{-1}, mainly as a result of the limited active adsorption sites covered by Cr(VI) ions on the adsorbent surface [4]. The removal capacity increased along with increasing the initial Cr(VI) concentration, indicating that the active sites were gradually saturated with the adsorbed Cr(VI) ions [11]. And also the increasing driving force provided by the higher initial Cr(VI) concentration on the NMC surface enabled more collisions between the Cr(VI) ions and active sites, and therefore resulted in a greater amount of Cr(VI) ions being adsorbed or reacted on the surface of NMC [20]. Figure 5b shows the effect of adsorbent concentration on the Cr(VI) removal. The increase of adsorbent loading can efficiently enhance the Cr(VI) removal, which

can be attributed to more active sites for the adsorption of Cr(VI) ions on the surface of adsorbent. The decrease of q_e demonstrated that most active sites were saturated [11]. A higher Cr(VI) removal efficiency was observed for the NMC (Figure 5c) with almost 90% Cr(VI) removal percentages with 7.5 mg g^{-1} (q_e) within 2.5 min, demonstrating that the NMC could be used as excellent adsorbents for the adsorption of Cr(VI) ions with high removal capacity and fast removal rate.

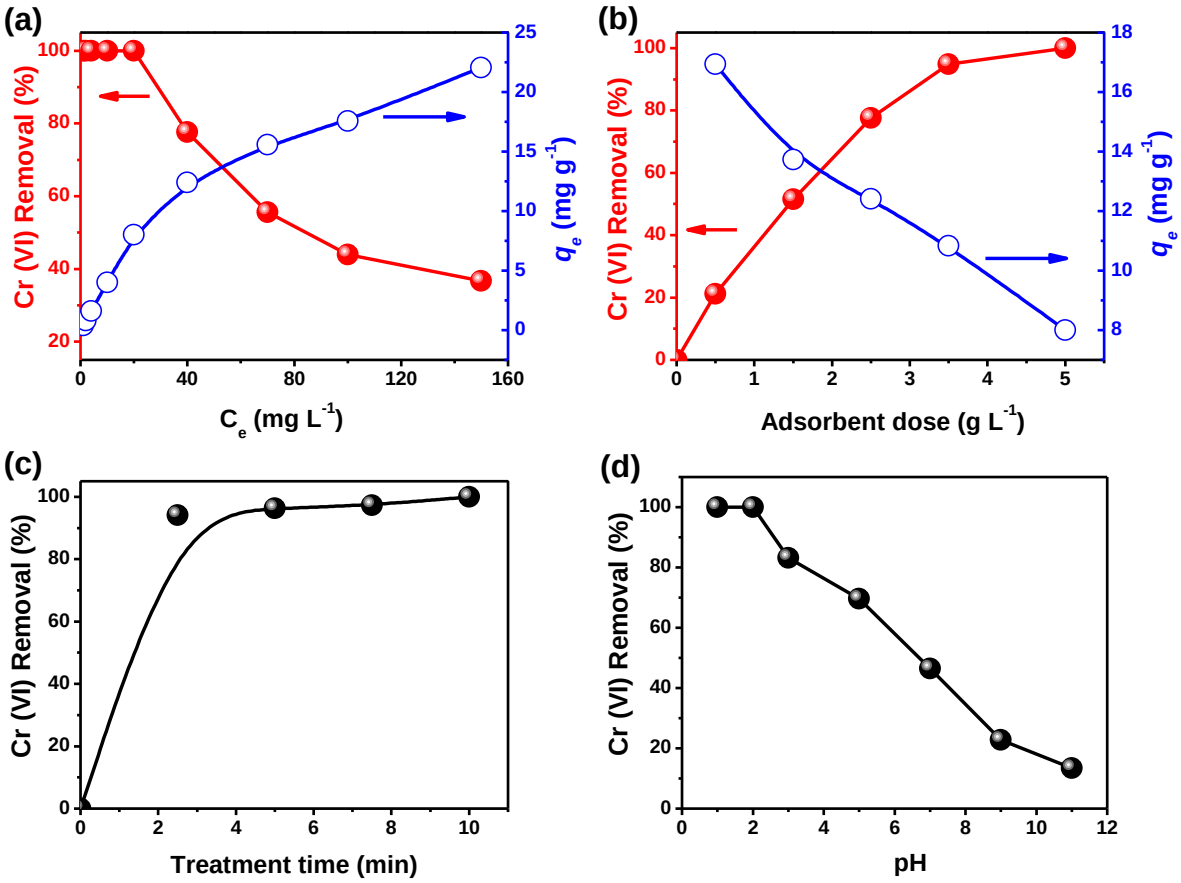

Figure 5. (a) effect of initial Cr(VI) concentration on Cr(VI) removal performance (adsorbent dosage: 50.0 mg, volume: 20 mL, pH: 7.0, treating time: 10 min) and the transformed rate plot C_e vs. q_e (open circle with blue color); (b) Cr(VI) removal performance of different adsorbent concentrations([Cr(VI)] = 40 mg L^{-1}, pH = 7.0, volume: 20 mL, treating time: 10 min) and the transformed rate plot C_e vs. q_e (open circle with blue color); (c) Cr(VI) removal performance with different treatment time ([Cr (VI)] = 40 mg L^{-1}, pH = 7, adsorbent dosage: 50.0 mg,

volume: 20 mL); (d) Effect of solution pH on the Cr(VI) removal efficiency of NMC. ([Cr(VI)] = 1000 mg L^{-1}, adsorbent dosage: 50.0 mg, volume: 20 mL, treating time: 10 min).

It has been shown that pH plays an important role on the heavy metal ion removal [4]. In this work, NMC was added into solutions with an initial Cr(VI) concentration of 1000 mg L^{-1} and a wide range of pH from 1 to 11 (Figure 5d). The removal percentage of Cr(VI) increased from 46.5% to 100% when the pH changed from 7.0 to 1.0, demonstrating the Cr(VI) removal enhancement with a strong acidic medium. When the pH value increased from 7 to 11, a negative effect on Cr(VI) removal was observed (from 46.5% to 13.4%). Cr(VI) ions could exist in several anionic forms (i.e.,$Cr_2O_7^{2-}$, $HCr_2O_7^-$, $HCrO_4^-$ and CrO_4^{2-}) in aqueous solutions [4, 11]. At a lower pH (< 6.8), the main species is $HCrO_4^-$, while CrO_4^{2-} will be the dominating specie when pH is above 6.8 [11]. In addition, the surface chemistry of adsorbent plays a key role in the Cr(VI) removal efficiency. As reported by Zhang et al., the pH at point of zero charge (pH_{pzc}) of NMC is about 3.6, much lower than the regular carbon materials, for instance, granular activated carbon (6.3), natural corncob (6.2), and untreated coffee husks (4.5) [20, 40-42]. The low pH_{pzc} was beneficial for the negative charge on the surface of NMC and thus enhanced the adsorption of Cr(VI) ions [18, 20]. With increasing the pH, the Cr(VI) removal percentage gradually decreased, arising from the adsorption competition between the highly concentrated OH^- ions and Cr(VI) ions. In addition, the electrostatic repulsion between the Cr(VI) ions and the active sites on the surface of NMC would increase when the pH was over pH_{pzc} of NMC [20], indicating more difficult for the NMC to adsorb Cr(VI) ions in the alkaline solution.

Two kinetic models (i.e., pseudo-first-order and pseudo-second-order models) were employed in this work (Figure S5). The adsorption process was found to fit better with a pseudo-second-order model with a correlation more than 0.99, indicating a chemical adsorption for the NMC adsorbents [43]. The adsorption isotherms fitted by Langmuir and Freundlich

models of Cr(VI) ions on the surface of NMC were obtained in neutral and acidic solutions (Figure S6 and Table S3). The calculated maximum Cr(VI) removal capacity based on the Langmuir model was about 29.46 and 2001.4 mg g^{-1} in neutral and acidic solutions, much higher than the reported adsorbents, and displayed competitive performance to the adsorbent (such as nano Fe, activated carbon and α-Fe_2O_3) in the acidic circumstance (see Table 3) [23, 44, 45]. The NMC in this work displayed higher q_{max} and q_s than the reported nitrogen doped magnetic carbons even though our NMCs had lower surface areas, which could be attributed to more active sites created on the surface after nitrogen doping [18, 20, 46].

Table 3 Comparison of Cr(VI) removal capacities with other adsorbents.

	Adsorbent	S_{BET} (m^2 g^{-1})	q_{max} [a] (mg g^{-1})	q_s [b] (mg m^{-2})	pH	Refs.
Neutral solution	NMC-100	56.2	29.46	0.52	7	**This work**
	Magnetic Carbon (Cellulose)	111.4	15.3	0.14	7	[4]
	MN (Cotton fabric)	91.1	3.74	0.04	7	[11]
	Graphene nanocomposites	42.1	1.03	0.02	7	[47]
Acidic solution	NMC-100	56.2	2001.4	35.61	1	**This work**
	N-doped porous carbon (Fe)	1136.0	16	0.02	3	[18]
	N-doped porous carbon (Ni)	2148.4	96.27	0.04	2.5	[20]
	Melamine–resorcinol–terephthaldehyde (MRT)	628.0	102.88	0.16	3	[23]
	Micron Fe	–	2.16-1.33	–	3	[48]
	Nano Fe	35	64.16-67.67	1.83-1.93	3	[48]
	α-Fe_2O_3	40.0	4.47	0.11	3	[44]
	Activated carbon	n/a	112.36	n/a	1	[45]
	MnO_2/Fe_3O_4/o-WCNTs	92.0	186.9	2.03	2	[49]

[a] q_{max} is obtained through the Langmuir isotherm; [b] q_s is represented as the adsorption capacity per m^2 of catalyst surface.

3.3 *Reusability*

The reusability of adsorbent is an important consideration for practical applications. Figure 6 shows the stability of the NMC in the Cr(VI) removal for five runs. After each run,

the recycled adsorbent was washed by deionized water and 0.01 mol L^{-1} NaOH solution repeated several times for the adsorbent regeneration [49, 50]. After that, the adsorbent was then dried at 80 ^{o}C overnight. The results demonstrated that the adsorbents displayed only a slight decline in the Cr(VI) removal when used 5 times. About 90% removal percentage of Cr(VI) and 7.5 mg g^{-1} removal capacity for the 5th cycle were obtained, demonstrating an excellent stability for the Cr(VI) removal over NMC under mild conditions. The declined activity can be attributed to the consumption of zero-valence iron and the blocked active sites by the adsorbed Cr(VI) and Cr(III) ions (Figure 7a) [18]. showed The obtained similar I_D/I_G values in the Raman spectra before and after usage (Figure 7b) indicate that the adsorbent was very stable in natural solution for the Cr(VI) removal. Additionally, the saturation magnetizations of fresh and used adsorbents were 130.7 and 125.8 emu g^{-1}, respectively, and thus could be easily separated by the permanent magnet from the treated solution after usage (Figure 7c). The slight decrease of adsorbent magnetizaiton was possibly caused by the comsuption of the ZVI, forming the iron oxide and Cr(III) ions on the surface of adsorbent [4]. The Fe 2p XPS spectra of the adsorbent before and after used were shown in Figure 7d. Four main peaks, i.e., the ZVI (706.9 eV), Fe^{2+} (709.8 eV) and Fe^{3+} (711.8 eV and 724.7 eV), were deconvoluted. Compared with the fresh adsorbent, almost no ZVI particles were observed after 5 times recycles, indicating that the ZVI was consumed during the treatment process. These results demonstrated that the NMC displayed an excellent structrure and performance stability under the current condition.

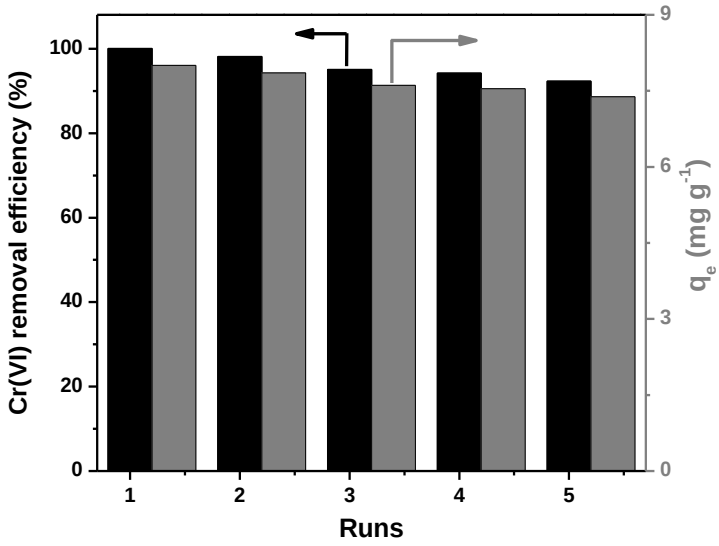

Figure 6. The reusability of the NMC for the Cr(VI) removal in this work, condition: [Cr (VI)] = 20 mg L^{-1}, pH = 7.0, adsorbent dosage: 50.0 mg, volume: 20 mL, treatment time: 10 min.

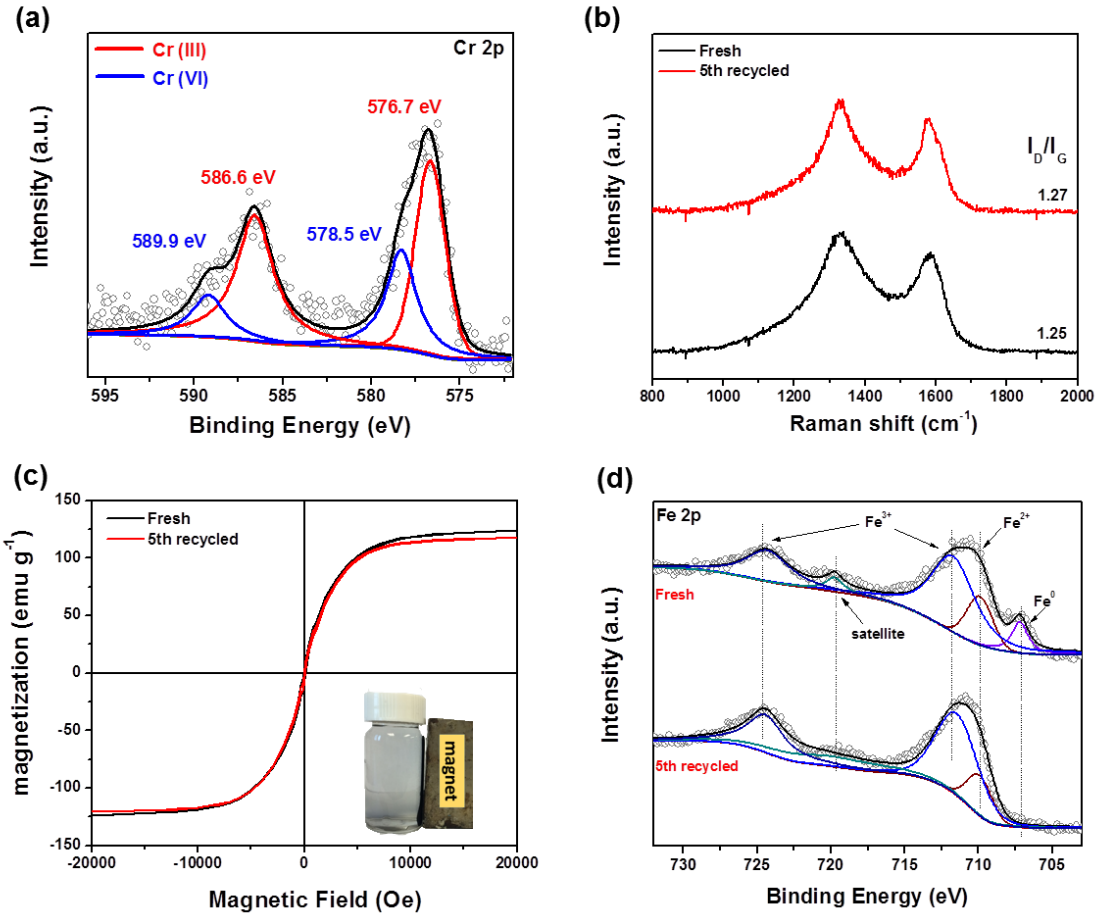

Figure 7. (a) Raman spectral, (b) magnetization and (c) Fe 2p XPS spectra of the fresh and 5th recycled samples, (d) Cr 2p XPS result of the 5th recycled samples.

3.4 *Removal mechanism of NMC*

According to earlier results, magnetic carbons can efficiently remove Cr(VI) ions through two key pathways: adsorption and redox reaction [47]. The redox reaction between the ZVI and Cr(VI) took place following equation (3):[4]

$$Cr_2O_7^{2-} + 2Fe + 7H_2O \rightarrow 2Cr^{3+} + 2Fe^{3+} + 14OH^- \quad (3)$$

In this study, the ZVI also existed on the surface of samples (Figure 2). From the XPS result, similar Fe contents were obtained on the MC and NMC (Table S1). Nevertheless, much higher activity was observed over nitrogen doped adsorbents (Table 2). Neverthless, there is rare work focusing on the structure and heteroatoms functionality on the surface of adsorbent. In order to investigate the relationship between the Cr(VI) removal and physical/chemical properties of adsorbents in details, the NMC with different nitrogen contents and other physical properties were prepared to investigate the structure-performance relationship for the Cr(VI) removal.

The role of nitrogen content on the Cr(VI) removal was investigated to obtain an intrinsic mechanism for the Cr(VI) removal. The nitrogen content in magnetic carbons was tuned by the glucose adding. The Cr(VI) removal performance with different NMCs are shown in the Figure 8. The nitrogen doping apparently enhanced the Cr(VI) removal performance. In this work, with the increase of melamine, the sole nitrogen source, the Cr(VI) removal percentages gradually increased (Figure 8a). The highest efficiency for the Cr(VI) removal was obtained on the NMC-100, displaying 100% removal for the 20 mg L^{-1} Cr(VI) concentration within 10 min. Moreover, larger BET specific surface area and bigger pore size not only benefited the adsorption of Cr(VI) ions (See Figure S7), but also improved the Cr(VI) diffusion into the internal pores and thereby facilitated the redox reaction with the electron donors (i.e., ZVI and

Cr(VI) ions) [4]. Furthermore, in this study, the defect of NMCs was observed not the vital factor in the Cr(VI) removal (Figure S8). To exclude the effect of the structure dependence, the removal rate normalized by mass weight and surface area were applied to represent the Cr(VI) removal efficiency. From the Figure 8b, the removal rates based on the mass and specific surface areas also increased with increasing the nitrogen dopant. The highest removal activity, 0.057 mg m^{-2} min^{-1}, was obtained over the adsorbent synthesized from melamine (NMC-100). These results evidently showed that the removal activity of NMCs could be modulated by the nitrogen doping level.

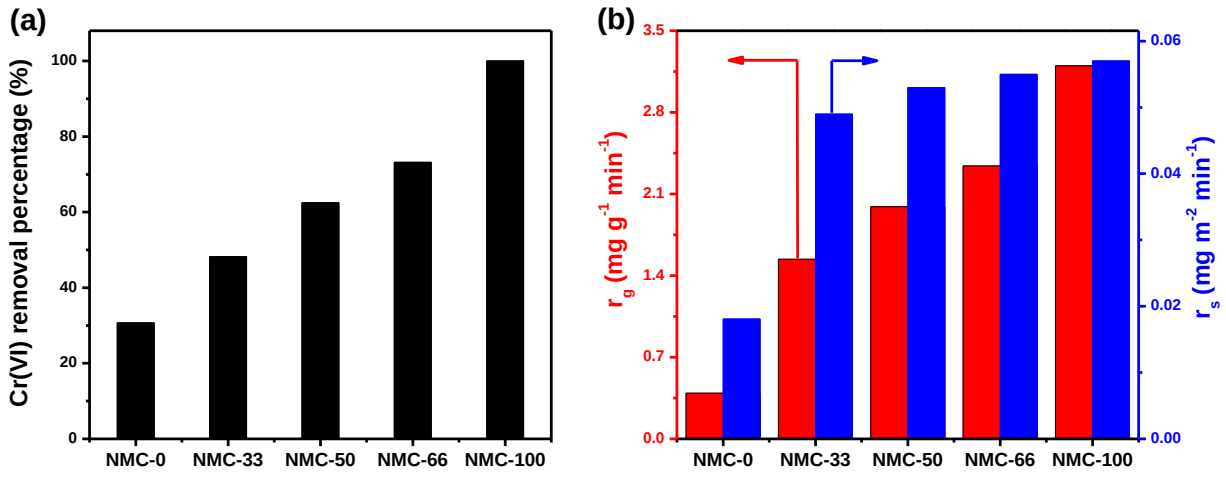

Figure 8. [a] Performance of different adsorbents on the Cr(VI) removal, condition: [Cr (VI)] = 20 mg L^{-1}, pH = 7.0, adsorbent dosage: 50.0 mg, volume: 20 mL, treatment time: 10 min; [b] Removal rate of Cr(VI) per gram and per m^2 of catalyst surface of adsorbent based on the treatment within 2.5 min.

The specific type of the nitrogen functionalities on the surface of NMC, such as pyridinic and quaternary nitrogen, are usually considered as the active sites to adsorb the intermediate species [51, 52]. Therefore, it is necessary to obtain the effect of specific nitrogen functionalities for the Cr(VI) removal. Figure 9 shows the dependences of surface-area-normalized activity on the nitrogen gross content and functionalities content in NMCs. The results demonstrated that the nitrogen dopant acted as active sites on the surface and could

directly enhance the Cr(VI) removal. This indicated that the negative charge of nitrogen dopant was much helpful for the adsorption of Cr(VI) ions, displaying a positive effect of nitrogen heteroatoms on the Cr(VI) removal [18, 20]. Therefore, it can be concluded that the Cr(VI) removal activity can be efficiently adjusted by the nitrogen dopant.

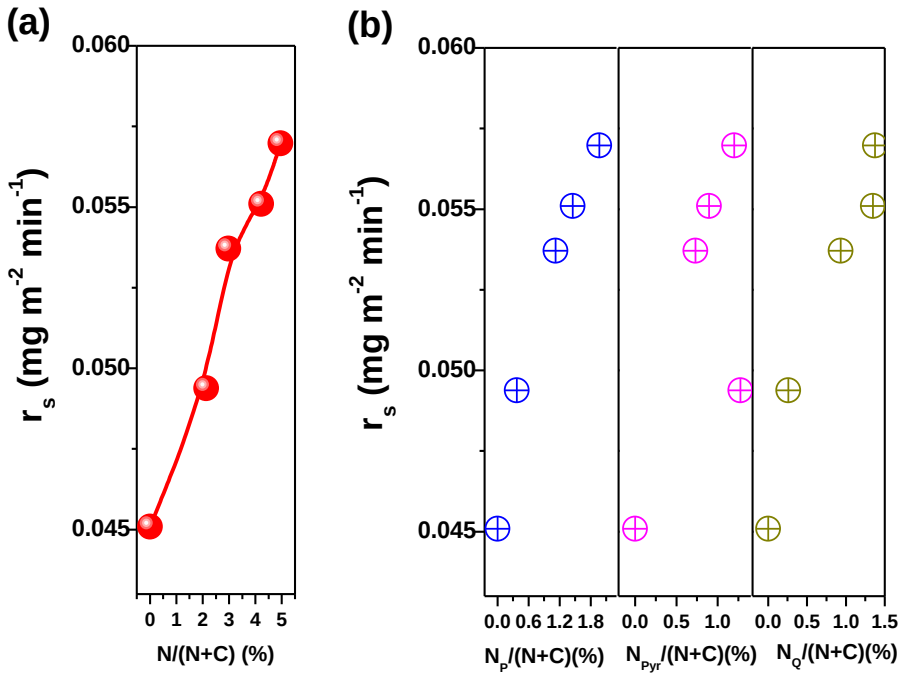

Figure 9. Dependences of Cr(VI) removal rate on the amounts of nitrogen: (a) gross N content; (b) N functionalities, N_P: pyridinic group; N_{pyr}: pyrrolic group; N_Q: graphitic N group.

To further understand the important role of adsorbent in the heavy metal removal, the DFT simulation was usually utilized to faciliate further undertanding the interaction between the adsorbent and metal ions [53, 54]. In this work, the MC and NMC displayed huge differences on the Cr(VI) removal and N dopant was proved to greatly enhance the Cr(VI) removal performance. Since the nitrogen dopant can change the surface charge density of nanocarbons, we believed that the attraction between the CrO_4^{2-} and adsorbent can be adjusted after the addition of nitrogen dopant. As repoted that CrO_4^{2-} is the main chromium species in the nuetral solution, herein we selected CrO_4^{2-} species represented as the Cr(VI) ion [4, 11]. As shown in

the Figure 10, the CrO_4^{2-} ions was attracted by the adsorbent due to the electrostatic attraction [4]. And then the CrO_4^{2-} reacted with the ZVI particles through the redox reaction to produce Cr(III) ions, whcih was also adsorbed on the surface of adsorbent. The interaction between the adsorbents and metal ions played a significant role on enhancing the Cr(VI) removal efficiency. The DFT results demonstrated that the adsorption energy for the MC and NMC to adsorb CrO_4^{2-} ions was -3.344 and -3.456 kJ mol^{-1}, respectively, demonstrating that the NMC could adsorb the CrO_4^{2-} ions more easily, consistent with our experimental results (Table 2), revealling that N doping efficiently facilitated the Cr(VI) removal by the enhanced interaction between metal ions and carbons.

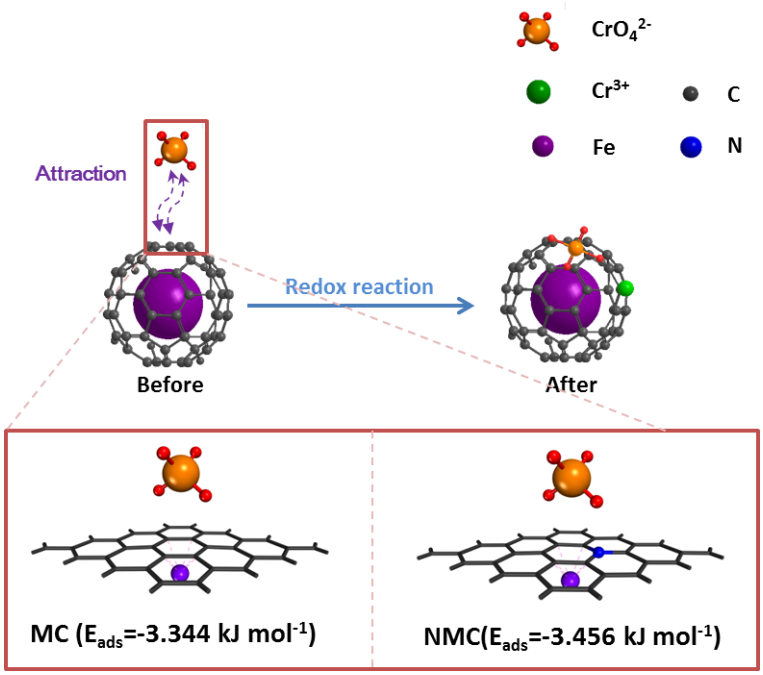

Figure 10. Proposed adsorption mechanism of magnetic carbons for the Cr(VI) removal.

4. Conclusions

In this work, NMCs synthesized from melamine have demonstrated as unique adsorbents for the Cr(VI) removal. The N dopant can modulate the physical/chemistry property of the adsorbents, such as morphology, defects and surface functionality. A systematic investigation on the influences of the N content, pH, Cr(VI) concentration, treatment time and adsorbent

dose showed that excellent Cr(VI) removal performance can be attributed to the nitrogen dopant and the ZVI. The N dopant on the carbon surface can increase its negative charge density and then enhance the ability for the Cr(VI) removal rate (3.20 mg g^{-1} min^{-1}), much higher than the undoped sample (0.98 mg g^{-1} min^{-1}). The Cr(VI) removal capacity of 29.4 and 2001.4 mg g^{-1} for the neutral and acidic solution, respectively, was obtained over NMC. The DFT theoretical calculation results also revealed a lower adsorption energy (-3.456 kJ mol^{-1}) between the NMC and metal ions than the undoped one (-3.344 kJ mol^{-1}), evidencing that the nitrogen dopant could enhance the interation between the metal ions and adsorbent. In addition, the NMC with outstanding recyclability have demonstraed excellent potential adsorbent for serving as nanoadorbents.

5. Supporting Information Available.

Additional characterization, adsorption kinetic study and more discussion can be found in Supporting Information.

Acknowledgments

This project was financially supported from the start-up fund of University of Tennessee, National Natural Science Foundation of China (Nos. 21503082, 51573063 and 21174044), Guangdong Provincial National Science Foundation (Nos. 2014A030310447 and S2013020013855), Fundamental Research Funds for the Central Universities of China (No. 2015ZM048), Guangdong Science and Technology Planning Project (Nos. 2014B010104004, 201604010013 and 2013B090600126) and National Basic Research Development Program 973 in China (NO. 2012CB025902). J. Huang acknowledges the support from China Scholarship Council (CSC) program. Part of the characterizations including the TGA, TEM

and XRD were carried out at the Center for Nanophase Materials Sciences, which is a DOE Office of Science User Facility.

References

[1] P. Suksabye, A. Nakajima, P. Thiravetyan, Y. Baba, W. Nakbanpote. Mechanism of Cr(VI) adsorption by coir pith studied by ESR and adsorption kinetic. J. Hazard. Mater. 2009; 161 (2–3): 1103-8.

[2] L.C. Hsu, S.L. Wang, Y.C. Lin, M.K. Wang, P.N. Chiang, J.C. Liu, et al. Cr(VI) Removal on Fungal Biomass of Neurospora crassa: the Importance of Dissolved Organic Carbons Derived from the Biomass to Cr(VI) Reduction. Environ. Sci. Tech. 2010; 44 (16): 6202-8.

[3] Z. Wei, R. Xing, X. Zhang, S. Liu, H. Yu, P. Li. Facile Template-Free Fabrication of Hollow Nestlike α-Fe2O3 Nanostructures for Water Treatment. ACS Appl. Mat. Interfaces 2013; 5 (3): 598-604.

[4] B. Qiu, H. Gu, X. Yan, J. Guo, Y. Wang, D. Sun, et al. Cellulose derived magnetic mesoporous carbon nanocomposites with enhanced hexavalent chromium removal. J. Mater. Chem. A 2014; 2 (41): 17454-62.

[5] B. Krishna, D. Murty, B.J. Prakash. Surfactant-modified clay as adsorbent for chromate. Appl. Clay Sci. 2001; 20 (1): 65-71.

[6] A.M. Yusof, N.A.N.N. Malek. Removal of Cr(VI) and As(V) from aqueous solutions by HDTMA-modified zeolite Y. J. Hazard. Mater. 2009; 162 (2): 1019-24.

[7] D. Kratochvil, P. Pimentel, B. Volesky. Removal of trivalent and hexavalent chromium by seaweed biosorbent. Environ. Sci. Tech. 1998; 32 (18): 2693-8.

[8] A. Szabó, D. Gournis, M.A. Karakassides, D. Petridis. Clay−Aminopropylsiloxane Compositions. Chem. Mater. 1998; 10 (2): 639-45.

[9] H. Tamai, T. Kakii, Y. Hirota, T. Kumamoto, H. Yasuda. Synthesis of Extremely Large Mesoporous Activated Carbon and Its Unique Adsorption for Giant Molecules. Chem. Mater. 1996; 8 (2): 454-62.

[10] B. Qiu, Y. Wang, D. Sun, Q. Wang, X. Zhang, B.L. Weeks, et al. Cr(VI) removal by magnetic carbon nanocomposites derived from cellulose at different carbonization temperatures. J. Mater. Chem. A 2015; 3 (18): 9817-25.

[11] J.H. Zhu, H.B. Gu, J. Guo, M.J. Chen, H.G. Wei, Z.P. Luo, et al. Mesoporous magnetic carbon nanocomposite fabrics for highly efficient Cr(VI) removal. J. Mater. Chem. A 2014; 2 (7): 2256-65.

[12] I.L. Shashkova, A.I. Rat'ko, N.V. Kitikova. Removal of heavy metal ions from aqueous solutions by alkaline-earth metal phosphates. Colloids Surf., A 1999; 160 (3): 207-15.

[13] C.X. Xu, B. Qiu, H.B. Gu, X.R. Yang, H.G. Wei, X.H. Huang, et al. Synergistic Interactions between Activated Carbon Fabrics and Toxic Hexavalent Chromium. ECS J. Solid State Sci. Technol. 2014; 3 (3): M1-M9.

[14] J.H. Zhu, S.Y. Wei, M.J. Chen, H.B. Gu, S.B. Rapole, S. Pallavkar, et al. Magnetic nanocomposites for environmental remediation. Adv. Powder Technol. 2013; 24 (2): 459-67.

[15] J.H. Zhu, R. Sadu, S.Y. Wei, D.H. Chen, N. Haldolaarachchige, Z.P. Luo, et al. Magnetic Graphene Nanoplatelet Composites toward Arsenic Removal. ECS J. Solid State Sci. Technol. 2012; 1 (1): M1-M5.

[16] X. Lv, X. Xue, G. Jiang, D. Wu, T. Sheng, H. Zhou, et al. Nanoscale Zero-Valent Iron (nZVI) assembled on magnetic Fe3O4/graphene for Chromium (VI) removal from aqueous solution. J. Colloid Interface Sci. 2014; 417: 51-9.

[17] F. Cai, X. Liu, S. Liu, H. Liu, Y. Huang. A simple one-pot synthesis of highly fluorescent nitrogen-doped graphene quantum dots for the detection of Cr(VI) in aqueous media. RSC Adv. 2014; 4 (94): 52016-22.

[18] Y. Li, S. Zhu, Q. Liu, Z. Chen, J. Gu, C. Zhu, et al. N-doped porous carbon with magnetic particles formed in situ for enhanced Cr(VI) removal. Water Res. 2013; 47 (12): 4188-97.

[19] K.-Y. Shin, J.-Y. Hong, J. Jang. Heavy metal ion adsorption behavior in nitrogen-doped magnetic carbon nanoparticles: Isotherms and kinetic study. J. Hazard. Mater. 2011; 190 (1-3): 36-44.
[20] S. Zhang, X. Wang, J. Li, T. Wen, J. Xu, X. Wang. Efficient removal of a typical dye and Cr(VI) reduction using N-doped magnetic porous carbon. RSC Adv. 2014; 4 (108): 63110-7.
[21] G. Zhao, L. Jiang, Y. He, J. Li, H. Dong, X. Wang, et al. Sulfonated graphene for persistent aromatic pollutant management. Adv. Mater. 2011; 23 (34): 3959-63.
[22] A.L. Allred, E.G. Rochow. A scale of electronegativity based on electrostatic force. J. Inorg. Nucl. Chem. 1958; 5 (4): 264-8.
[23] J. Wang, S. Xu, Y. Wang, R. Cai, C. Lv, W. Qiao, et al. Controllable synthesis of hierarchical mesoporous/microporous nitrogen-rich polymer networks for CO_2 and Cr(VI) ion adsorption. RSC Adv. 2014; 4 (31): 16224-32.
[24] F. Lin, Y. Wang, Z. Lin. One-pot synthesis of nitrogen-enriched carbon spheres for hexavalent chromium removal from aqueous solution. RSC Adv. 2016; 6 (39): 33055-62.
[25] H. Kruse, L. Goerigk, S. Grimme. Why the Standard B3LYP/6-31G* Model Chemistry Should Not Be Used in DFT Calculations of Molecular Thermochemistry: Understanding and Correcting the Problem. J. Org. Chem. 2012; 77 (23): 10824-34.
[26] R. Zhang, L. Ling, Z. Li, B. Wang. Solvent effects on Cu2O(1 1 1) surface properties and CO adsorption on Cu2O(1 1 1) surface: A DFT study. Appl. Catal. A: Gen 2011; 400 (1–2): 142-7.
[27] N. Zhao, S. Wu, C. He, Z. Wang, C. Shi, E. Liu, et al. One-pot synthesis of uniform Fe3O4 nanocrystals encapsulated in interconnected carbon nanospheres for superior lithium storage capability. Carbon 2013; 57: 130-8.
[28] G. Zhong, H. Wang, H. Yu, F. Peng. Nitrogen doped carbon nanotubes with encapsulated ferric carbide as excellent electrocatalyst for oxygen reduction reaction in acid and alkaline media. J. Power Sources 2015; 286 (0): 495-503.
[29] J.-S. Li, S.-L. Li, Y.-J. Tang, M. Han, Z.-H. Dai, J.-C. Bao, et al. Nitrogen-doped Fe/Fe3C@graphitic layer/carbon nanotube hybrids derived from MOFs: efficient bifunctional electrocatalysts for ORR and OER. Chem. Commun. 2015; 51 (13): 2710-3.
[30] J.R. Pels, F. Kapteijn, J.A. Moulijn, Q. Zhu, K.M. Thomas. Evolution of nitrogen functionalities in carbonaceous materials during pyrolysis. Carbon 1995; 33 (11): 1641-53.
[31] B. Stöhr, H.P. Boehm, R. Schlögl. Enhancement of the catalytic activity of activated carbons in oxidation reactions by thermal treatment with ammonia or hydrogen cyanide and observation of a superoxide species as a possible intermediate. Carbon 1991; 29 (6): 707-20.
[32] Z. Chen, D. Higgins, H.S. Tao, R.S. Hsu, Z.W. Chen. Highly Active Nitrogen-Doped Carbon Nanotubes for Oxygen Reduction Reaction in Fuel Cell Applications. J. Phys. Chem. C 2009; 113 (49): 21008-13.
[33] S. Van Dommele, A. Romero-Izquirdo, R. Brydson, K.P. de Jong, J.H. Bitter. Tuning nitrogen functionalities in catalytically grown nitrogen-containing carbon nanotubes. Carbon 2008; 46 (1): 138-48.
[34] Y. Cao, H. Yu, J. Tan, F. Peng, H. Wang, J. Li, et al. Nitrogen-, phosphorous-and boron-doped carbon nanotubes as catalysts for the aerobic oxidation of cyclohexane. Carbon 2013; 57: 433-42.
[35] S. Maldonado, S. Morin, K.J. Stevenson. Structure, composition, and chemical reactivity of carbon nanotubes by selective nitrogen doping. Carbon 2006; 44 (8): 1429-37.
[36] D. Price, Y. Liu, G.J. Milnes, R. Hull, B.K. Kandola, A.R. Horrocks. An investigation into the mechanism of flame retardancy and smoke suppression by melamine in flexible polyurethane foam. Fire Mater. 2002; 26 (4-5): 201-6.
[37] M.J. Alowitz, M.M. Scherer. Kinetics of Nitrate, Nitrite, and Cr(VI) Reduction by Iron Metal. Environ. Sci. Tech. 2002; 36 (3): 299-306.

[38] R.-S. Juang, M.-L. Chen. Application of the Elovich Equation to the Kinetics of Metal Sorption with Solvent-Impregnated Resins. Ind. Eng. Chem. Res. 1997; 36 (3): 813-20.
[39] S.K. Srivastava, R. Tyagi, N. Pant. Adsorption of heavy metal ions on carbonaceous material developed from the waste slurry generated in local fertilizer plants. Water Res. 1989; 23 (9): 1161-5.
[40] T. Karanfil, J.E. Kilduff. Role of Granular Activated Carbon Surface Chemistry on the Adsorption of Organic Compounds. 1. Priority Pollutants. Environ. Sci. Tech. 1999; 33 (18): 3217-24.
[41] L. Billon, V. Meric, A. Castetbon, J. Francois, J. Desbrieres. Removal of copper ions from water of boilers by a modified natural based, corncobs. J. Appl. Polym. Sci. 2006; 102 (5): 4637-45.
[42] L.C.A. Oliveira, R.V.R.A. Rios, J.D. Fabris, V. Garg, K. Sapag, R.M. Lago. Activated carbon/iron oxide magnetic composites for the adsorption of contaminants in water. Carbon 2002; 40 (12): 2177-83.
[43] J.H. Zhu, H.B. Gu, S.B. Rapole, Z.P. Luo, S. Pallavkar, N. Haldolaarachchige, et al. Looped carbon capturing and environmental remediation: case study of magnetic polypropylene nanocomposites. RSC Adv. 2012; 2 (11): 4844-56.
[44] L.S. Zhong, J.S. Hu, H.P. Liang, A.M. Cao, W.G. Song, L.J. Wan. Self-Assembled 3D Flowerlike Iron Oxide Nanostructures and Their Application in Water Treatment. Adv. Mater. 2006; 18 (18): 2426-31.
[45] A. El-Sikaily, A.E. Nemr, A. Khaled, O. Abdelwehab. Removal of toxic chromium from wastewater using green alga Ulva lactuca and its activated carbon. J. Hazard. Mater. 2007; 148 (1–2): 216-28.
[46] A. Modi, B. Bhaduri, N. Verma. Facile One-Step Synthesis of Nitrogen-Doped Carbon Nanofibers for the Removal of Potentially Toxic Metals from Water. Ind. Eng. Chem. Res. 2015; 54 (18): 5172-8.
[47] J.H. Zhu, S.Y. Wei, H.B. Gu, S.B. Rapole, Q. Wang, Z.P. Luo, et al. One-Pot Synthesis of Magnetic Graphene Nanocomposites Decorated with Core@Double-shell Nanoparticles for Fast Chromium Removal. Environ. Sci. Tech. 2012; 46 (2): 977-85.
[48] J. Cao, W.-X. Zhang. Stabilization of chromium ore processing residue (COPR) with nanoscale iron particles. J. Hazard. Mater. 2006; 132 (2–3): 213-9.
[49] C. Luo, Z. Tian, B. Yang, L. Zhang, S. Yan. Manganese dioxide/iron oxide/acid Oxidized multi-walled carbon nanotube magnetic nanocomposite for enhanced hexavalent chromium removal. Chem. Eng. J. 2013; 234: 256-65.
[50] J. Wang, K. Pan, Q. He, B. Cao. Polyacrylonitrile/polypyrrole core/shell nanofiber mat for the removal of hexavalent chromium from aqueous solution. J. Hazard. Mater. 2013; 244–245: 121-9.
[51] Y. Gao, G. Hu, J. Zhong, Z. Shi, Y. Zhu, D.S. Su, et al. Nitrogen-doped sp2-hybridized carbon as a superior catalyst for selective oxidation. Angew. Chem. Int. Ed. 2013; 52 (7): 2109-13.
[52] C.L. Chen, J. Zhang, B.S. Zhang, C.L. Yu, F. Peng, D.S. Su. Revealing the enhanced catalytic activity of nitrogen-doped carbon nanotubes for oxidative dehydrogenation of propane. Chem. Commun. 2013; 49 (74): 8151-3.
[53] H. Valencia, A. Gil, G. Frapper. Trends in the Adsorption of 3d Transition Metal Atoms onto Graphene and Nanotube Surfaces: A DFT Study and Molecular Orbital Analysis. J. Phys. Chem. C 2010; 114 (33): 14141-53.
[54] A. Ishii, M. Yamamoto, H. Asano, K. Fujiwara. DFT calculation for adatom adsorption on graphene sheet as a prototype of carbon nanotube functionalization. J. Phys: Conf. Ser. 2008; 100 (5): 052087.